Clays and Clay Minerals, Vol. 48, No. 2, 159–172, 2000.

THE EFFECT OF Al ON Fe OXIDES. XIX. FORMATION OF Al-SUBSTITUTED HEMATITE FROM FERRIHYDRITE AT 25°C AND pH 4 TO 7

UDO SCHWERTMANN,[1] JOSEF FRIEDL,[1] HELGE STANJEK,[1] AND DARRELL G. SCHULZE[2]

[1] Lehrstuhl für Bodenkunde, Technische Universität München, D-85350 Freising-Weihenstephan, Germany
[2] Agronomy Department, Purdue University, 1150 Lilly Hall, West Lafayette, Indiana 47907-1150, USA

Abstract—Iron oxides in surface environments generally form at temperatures of 25 ± 10°C, but synthesis experiments are usually done at higher temperatures to increase the rate of crystallization. To more closely simulate natural environments, the transformation of 2-line ferrihydrite to hematite and goethite at 25°C in the presence of different Al concentrations and at pH values from 4 to 7 was studied in a long-term (16–20 y) experiment. Aluminum affects the hydrolysis and charging behavior of 2-line ferrihydrite and retards crystallization. Al also promotes the formation of hematite over goethite and leads to multidomainic discoidal and framboidal crystals instead of rhombohedral crystals. The strong hematite-promoting effect of Al appears to be the result of a lower solubility of the Al-containing ferrihydrite precursor relative to pure ferrihydrite. Hematite incorporates Al into its structure, as is shown by a decrease in the *a* and *c*-cell lengths and a decrease in magnetic hyperfine fields (Mössbauer spectroscopy). With hematite formed at low-temperature, these decreases were, however, smaller for the cell length and greater for the magnetic field than for hematite produced at higher temperatures. Both phenomena are removed by heating the hematite at 200°C. They are attributed to structural OH and/or structural defects. The relative content of Al in the structure is lower for hematite formed at 25°C than for hematites synthesized at higher temperatures (80 and 500°C). The maximum possible substitution of one sixth of the Fe positions was not achieved, similar to soil hematites. These results show that properties of widely distributed soil Al-containing hematites can reflect formation environment.

Key Words—Al-Substituted Hematite, Formation of Fe Oxide, Hyperfine Fields, Structural OH, Synthesis of Fe Oxides, Unit-Cell Size.

INTRODUCTION

Goethite and hematite are the most common Fe-oxide minerals in surface environments. Studies to determine the environmental conditions under which weathering and Fe-oxide formation occurs usually concentrate on three parameters: (1) the ratio of the amount of goethite to hematite, (2) the crystallinity of the two oxides, and (3) structural Al content. These parameters contain information relating to conditions of formation. The goethite/hematite ratio, for example, is affected by temperature, water activity, and pH (for a review see Cornell and Schwertmann, 1996) and thus, the goethite/hematite ratio provides information on these variables in the weathering environment.

Synthesis experiments under controlled conditions help to identify and quantify the relative importance of these factors during oxide genesis. However, synthesis experiments often involve temperatures of 70–100°C, high alkalinity (for goethite), or high acidity (for hematite) to obtain crystalline products within a few days (Schwertmann and Cornell, 1991). At temperatures near 25°C, a water activity of 1, and pH in the range of 3–8, as in many surface environments, oxide formation is comparatively slow. For example, the formation of goethite and hematite from ferrihydrite required several years in an Al-free system at 25°C and pH ranges from 2.5 to 10. Two goethite maxima, at pH 4 and 10, and a hematite maximum near pH 7–8 were found under these conditions (Schwertmann, unpubl.; see Figure 13.10 in Cornell and Schwertmann, 1996). The conversion to these crystalline products was more complete at the higher pH values.

Most soil goethite and hematite show Al-for-Fe substitution because Al sources are commonly available in the crystallization environment. The factors that determine the extent of substitution have been studied by synthesis, although for kinetic reasons, at high temperature, high pH, or both. The results may therefore differ from those found at the Earth's surface. For example, decreasing the temperature from 70 to 25°C at an OH concentration [OH] of 0.3 mol L^{-1} almost doubled Al substitution in goethite at a given Al concentration (see Figure 3.6 in Cornell and Schwertmann, 1996). In addition, the presence of Al affects the rate of formation, crystal size and shape, and the goethite/hematite ratio.

To more nearly approach conditions in surface environments, such as soils, we studied the formation of goethite and hematite from 2-line ferrihydrite at 25°C in the presence of Al at pH values from 4 to 7, both with and without electrolytes, over a period of ≤19.6 y. The long aging time was necessary to obtain sufficient crystallized material for characterization.

Copyright © 2000, The Clay Minerals Society

https://doi.org/10.1346/CCMN.2000.0480202 Published online by Cambridge University Press

Table 1. Experimental conditions.

Series no.	Total Fe + Al mol	Total volume L	Range of Al/(Al + Fe) mol mol^{-1}	pH	Temp °C	Coprecipitate (Co) Mech. mixture (MM)	Electrolytes present (P) absent (A)	Duration y
22	0.05–0.0575	1	0–1.0	7.65	25	Co	P	18.8/19.6[1]
22A	0.05–0.06	1	0–0.17	7	25	Co	P	17.4
22B	0.05–0.06	1	0–0.17	5	25	Co	P	17.5
29A	0.05	0.5	0–0.15	4;5;6;7	25	Co	A	16.2
29B	0.05	0.5	0–0.15	4;5;6;7	25	MM	A	16.2
57	0.015	0.25	0–0.35	7	80	Co	A	0.18

[1] For 0–0.15 and 0.20–0.40 Al/(Al + Fe), respectively.

MATERIALS AND METHODS

Sample preparation

Series 22; 22A, 22B. Series 22 was prepared to study the effect of Al over the range of Al/(Al + Fe) from 0 to 1 mol mol^{-1} at pH values of 5, 7, and 7.65. Increasing amounts of a 0.1 M $Al(NO_3)_3 \cdot 9H_2O$ were added to 50 mL volumes of 0.25 M $Fe(NO_3)_3 \cdot 9H_2O$ in 1-L polypropylene bottles, brought to pH 7.65 with KOH, and then distilled water was added to produce 1 L (series 22). The Al/(Al + Fe) mol ratio of the system, hereafter referred to as R_i ranged between 0–1 in 12 steps. In addition, two subseries were prepared with the same solutions but an R_i range of 0–0.17 mol mol^{-1} in nine steps and maintained at pH 7.0 (series 22A) and pH 5.0 (series 22B). The electrolytes were not removed from these series.

Series 29A, 29B. In series 29, we studied the effect of pH (4–7) and of coprecipitated *versus* mechanical mixtures of Fe and Al. To do so, 250 mL of the Fe- and Al-salt solutions described above were either coprecipitated by adding a NH_3 solution at a pH of 7.5 (series 29A) or precipitated separately at pH 7.5 and mixed mechanically afterwards (series 29B). In each case, R_i ranged from 0 to 0.15 mol mol^{-1} in five steps. The precipitates were dispersed by adding distilled water to a volume of 500 mL, then washed twice by centrifugation and the pH adjusted to 7.5 after each wash to prevent dispersion. Distilled water was added to the precipitates to make a 500 mL suspension and the pH adjusted to 4, 5, 6, or 7 with 0.1 M HNO_3 or dilute NH_3.

All series were kept at a constant temperature of 25°C in a controlled climate room for ≤19.6 y. The pH was measured occasionally (more often in the beginning and nine times in total), readjusted to the target pH, if necessary, and subsamples taken to follow the degree of transformation by determining oxalate soluble iron (Fe_o) and total iron (Fe_t) (Schwertmann, 1964).

Series 57. For comparison, a series prepared at 80°C, pH 7, and an aging time of 65 d was included using 200–160 mL of 0.1 M $Fe(NO)_3$ combined with 0–40 mL of 0.1 M $Al(NO_3)_3$ solutions to produce 11 different Al/(Fe + Al) ratios between 0–0.20 mol mol^{-1}. After termination of the experiments, the oxides were washed free of electrolytes (series 22) and freeze-dried. Table 1 summarizes the experimental conditions for the five series at 25°C and the series at 80°C.

Sample characterization

When electrolytes were present, such as in Series 22, the end product was flocculated and easily separated from the supernatant. When electrolytes were absent, however, such as in Series 29, the end product was partially dispersed, particularly at pH 4 and 5. These samples were centrifuged for 25 min at ~11,000 × g to separate the supernatant solution from the sediment. The solids were then dried at 40°C in an oven. Aliquots of selected supernatants were freeze-dried and the solids further characterized. Fe_t and total Al (Al_t) were determined after complete dissolution of a 1 mL aliquot of the suspension in 1 mL of concentrated HCl. To determine the Al and Fe in the hematite, the samples containing only hematite and no goethite were purified sequentially as follows using ~20 mg of material: Ferrihydrite was removed first by two 2-h extractions with 10 mL of 0.2 M oxalate solution in the dark, followed by centrifuge washing with 4 mL fresh oxalate. Solid $Al(OH)_3$ was then removed by a 1-h extraction with 15 mL of 1.25 M NaOH at 75°C, followed by three centrifuge washings with ~5 mL distilled water. The Al and Fe in the remaining solid were then determined after dissolving the solid in 8 mL of 6 M HCl at 75°C in a water bath and measuring Al and Fe by atomic absorption spectroscopy. If only hematite was present, as was the case for most samples, these values were considered as structural Al and expressed as the molar ratio, Al/(Al + Fe), hereafter referred to as R_s.

Samples were prepared for X-ray diffraction (XRD) by mixing with 10% Si powder as an internal Bragg-angle standard and then preparing backfilled powder mounts. XRD patterns were obtained using CoKα radiation with a Philips PW 1070/1820 goniometer equipped with a diffracted-beam graphite monochromator and a fixed 1° divergence slit. XRD patterns were obtained by step scanning from 10 to 80 °2θ in

https://doi.org/10.1346/CCMN.2000.0480202 Published online by Cambridge University Press

0.05 °2θ increments using a 20-s counting time. Rietveld methods were employed by using the RIETAN (Izumi, 1993) or the GUFI-WYRIET (Schneider and Dinnebier, 1991) software to obtain a line-width function and unit-cell lengths of hematite and goethite. Selected samples were heated to various temperatures (see Results) for further characterization.

Mössbauer spectra were recorded at room temperature and 4.2 K using a sinusoidal acceleration spectrometer equipped with a ^{57}Co in Rh source. An α-Fe foil was used for calibration. The spectra were fitted with sets of split Gaussian distributions of Lorentzian-shaped lines for the magnetic sextets and quadrupole doublets as described by Friedl and Schwertmann (1996). Fourier transform infrared (FTIR) spectra were obtained using a Nicolet Magna 550 instrument in the transmission mode using 1 mg of sample in 300 mg KBr. The resolution was 1.9 cm^{-1}. Micrographs from transmission electron microscopy (TEM) and scanning electron microscopy (SEM) were acquired at the Laboratorium für Elektronenmikroskopie, Physik, Weihenstephan with a Zeiss EM 10A/B instrument and a 360 S instrument (Cambridge Instruments), respectively.

Surface area and micropore volume were determined from 7 or 11 adsorption points in the relative pressure (p/p_0) range between 0.05–0.3 using an AUTOSORB-1 instrument (Quantachrome) with N_2 as adsorbate. The multi-point Brunauer-Emmet-Teller (BET) method and Dubinin-Radushkevich (DR) analysis of the Quantachrome software were applied. Samples were outgassed at 70°C and ~40 mTorr for at least 2 h. The BET constant, C, ranged from 43 to 153.

RESULTS AND DISCUSSION

Change in pH

The pH of the suspension changed by <0.7 pH units between readjustments to the target pH. For a target pH of <7, the pH decreased between readjustments, and the magnitude of decrease was greater for a lower target pH. For a target pH of ≥7, the pH increased occasionally. The pH fluctuation during the aging period, however, was always less than the difference between the target pH values, so that pH is considered a true variable in this experiment.

The change in pH values during the experiment is caused by the net effect of the release of protons owing to further hydrolysis of Fe(III) and/or Al and to desorption of OH^- adsorbed on the surface of ferrihydrite. Desorption of OH^- is substantiated by Lewis and Schwertmann (1980) who showed that significant OH^- desorbed during the transformation of high-surface-area ferrihydrite precipitated at pH 7 to lower-surface-area goethite and hematite. They also found that the release of OH was larger with the greater amount of OH added initially.

For all series, the magnitude of pH decrease between pH readjustments was larger when the Al concentration, [Al], was lower the in the system. From the lowest to the highest Al addition for the five [Al] levels in series 29A, the average pH difference was 0.38, 0.35, 0.26, 0.15, and 0.06 (180 values), whereas for the four Al levels in series 29B it was 0.31, 0.22, 0.17, and 0.13 (144 values). It seems, therefore, that Al in the system promotes the hydrolysis of Fe(III) during the initial precipitation, indicating interaction between the two metals. This result was first observed by Taylor (1988), who found that the precipitation of mixed Fe(III)-Al solutions required more OH^- to achieve the same pH than separate solutions. Thus, there is a higher degree of hydrolysis in the mixed system.

Conversion of ferrihydrite to hematite and goethite as a function of time

The degree of conversion of ferrihydrite to hematite and goethite was inferred from the decrease in Fe_o/Fe_t. The conversion of the first 90% or more of the ferrihydrite to better crystalline oxides followed pseudo-first order kinetics (not shown) as found earlier (Schwertmann, 1988), although the samples were not stirred continuously. Hence, once crystallization started, the crystallization rate decreased over time. The rate of decrease is probably a function of the remaining ferrihydrite concentration. The rate, based on first-order kinetics, is:

$$(Fe_o/Fe_t)_t = e^{-kt} \quad (1)$$

where t is time in years and k is the reaction rate (y^{-1}). For $t = 0$, $Fe_o/Fe_t = 1$. As Al in the system increased, however, Fe_o/Fe_t remained at 1 for a longer time before decreasing. This lag-time may be the nucleation time, which can be obtained by extrapolation of Equation (1) to $Fe_o/Fe_t = 1$. As seen from Figure 1a and 1b, both k and the lag-time strongly depend on R_i in the system; k decreased and the lag-time increased exponentially as R_i increased, indicating that both nucleation and crystal growth of hematite were retarded by Al in the system. A weaker effect on these two parameters originates from pH, as shown before (Schwertmann and Murad (1983).

State of flocculation and dispersion

Whereas the electrolyte-containing system (series 22, NH_4NO_3) was fully flocculated, part of the oxides in the electrolyte-free system (series 29) were in a sol state throughout the aging process. In general, the proportion of dispersed Fe and Al decreased with time. The proportion increased with decreasing pH and increasing Al in the system (Table 2). The effect of pH is consistent with the charging behavior of ferrihydrite, with the zero point of charge near pH 7–8. A marked

https://doi.org/10.1346/CCMN.2000.0480202 Published online by Cambridge University Press

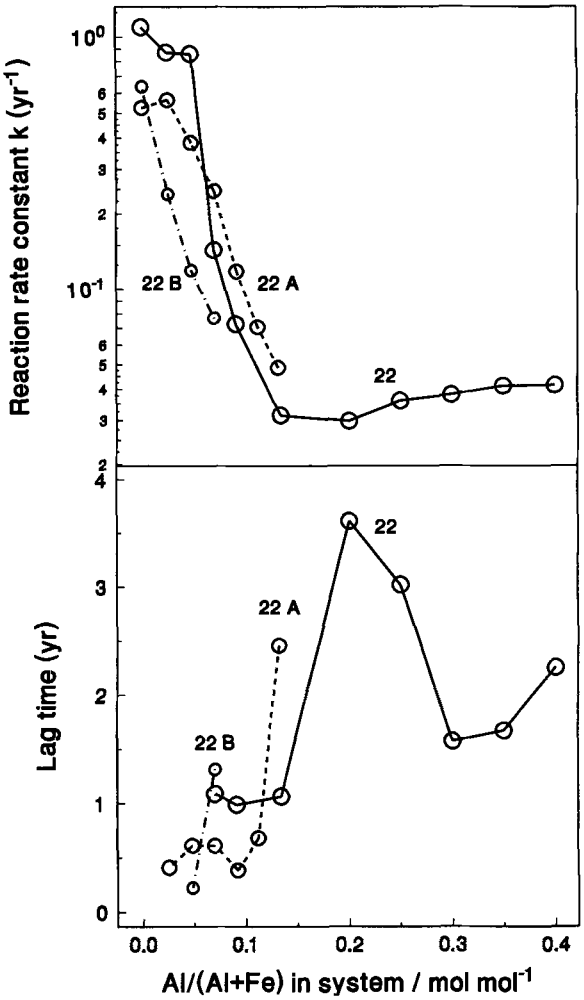

Figure 1. Reaction rate constant (a) and lag time (b) of the transformation of 2-line ferrihydrite to hematite-goethite as a function of Al/(Al + Fe) in the system (Series 22).

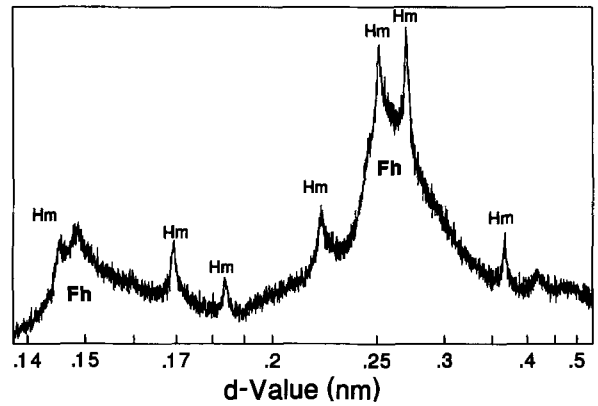

Figure 2. XRD of the freeze-dried 2-line ferrihydrite (Fh) sol after 17.5 y of aging at pH 4 with Al/(Al + Fe) of 0.15 mol mol^{-1} in the system (Series 29B) (Hm = hematite).

effect of Al was observed in both the coprecipitation (29A) and the mechanical mixture (29B) series which seems to affect the rate of crystallization of hematite. Taylor (1988) also observed a dispersive effect of Al on mixed Fe(III)-Al hydroxide precipitates. Increasing Al in the system leads to higher surface charging of the Al-containing ferrihydrite because it is more hydrolyzed (see above). An X-ray diffractogram of the freeze-dried sol showed only 2-line ferrihydrite after 16 y of aging with only a trace of hematite (Figure 2), which may have come from incomplete separation of the sol from the precipitate.

Thus, the sol state makes crystallization more difficult. This supports our concept that hematite formation from ferrihydrite requires prior aggregation of ferrihydrite to facilitate hematite nucleation and crystal growth (Fischer and Schwertmann, 1975; Schwertmann *et al.*, 1999). In contrast, dispersion limits the interaction between the ~3-nm sized, highly charged ferrihydrite particles and thereby hinders nucleation

Table 2. Proportion of Fe and Al in stable sol form after aging for 10.2 and 16.2 y.

Al/(Al + Fe) in system mol mol^{-1}	pH	After 10.2 y		After 16.2 y			
		Fe		Fe		Al	
		29A	29B	29A	29B	29A	29B
0	4	0.012		0.012	0	0	0
	5	0.018		0.005	0	0	0
	6	0		0.000	0	0	0
0.025	4	0.22	0.21	0.081	0.076	0.095	0.098
	5	0	0.14	8×10^{-4}	0.047	0	0.018
	6	0	0	10^{-4}	0.015	0	0.045
0.05	4	0.44	0.39	0.059	0.150	0.086	0.012
	5	0.43	0.31	0.112	0.105	0.114	0.082
	6	0	0	5×10^{-4}	0.096	0	0.10
0.10	4	0.71	0.68	0.28	0.30	0.36	0.035
	5	0.70	0.64	0.27	0.26	0.30	0.27
0.15	4	0.91	0.89	0.38	0.45	0.46	0.49
	5	0.70	0.54	0.34	0.34	0.39	0.26
	6	0	0	0	0.002	0	0.001

https://doi.org/10.1346/CCMN.2000.0480202 Published online by Cambridge University Press

and growth of hematite. Instead, goethite crystallizes slowly from a stable sol under strongly acid conditions (pH 1.5–2) (Atkinson *et al.,* 1968; Glasauer *et al.,* 1999).

Minerals formed

Hematite was the dominant or only crystalline phase in 56 of the 58 Al-containing samples. The following discussion therefore concentrates on hematite. Higher proportions of goethite (to 100%) were only formed in the seven Al-free systems and the two lowest Al members of series 22. The results occurred probably because of the relatively high pH (7.65), which favors goethite formation. The hematite/goethite ratios as determined by XRD are in general agreement with those obtained by Mössbauer spectra. Crystalline $Al(OH)_3$ phases occurred at high R_i but the occurrence also depended on pH and mode of preparation. Whereas no crystalline $Al(OH)_3$ was formed in the coprecipitated samples (series 29A), even at the highest R_i of 0.15 and pH 7, crystalline $Al(OH)_3$ did form in mechanical mixtures even at pH 5. Thus, Al is less available to form a separate hydroxide if coprecipitated with Fe than if mechanically mixed. In these, the three $Al(OH)_3$ polymorphs, gibbsite, bayerite, and nordstrandite, were identified by XRD but only gibbsite was present in the pure Al system (R_i of 1).

Hematite as the only oxide in most of the samples indicates that under our synthesis conditions small amounts of Al are effective in completely suppressing goethite formation in favor of hematite. The goethite-suppressing effect of Al has been reported from experiments at pH 7, but only at 70°C, where goethite is suppressed even at an R_i as low as 0.01 mol mol^{-1} (Schwertmann *et al.,* 1979). In contrast, at high pH ([OH] = 0.3 M) an R_i as high as 0.5 was needed to induce hematite formation at 25 and 70°C (Schulze and Schwertmann, 1987).

It is remarkable that even at ambient temperature and at a water activity of 1, hematite, the *anhydrous* phase, is so strongly favored over goethite, although goethite, the oxyhydroxide phase, is considered thermodynamically more stable in aqueous systems. Given sufficient time (*e.g.,* >10 y), hematite forms from ferrihydrite as a dominant phase in an Al-free system at a water activity of 1 at a temperature as low as 4°C (Schwertmann, unpubl.; see Figure 13.10 in Cornell and Schwertmann, 1996).

Ferrihydrite is a necessary precursor for hematite formation in the presence of water, at ambient temperatures and pH of approximately equal to or greater than three (Schwertmann *et al.,* 1999). Evidently, the lower the solubility of ferrihydrite, the more ferrihydrite is expected to direct crystallization towards hematite rather than towards goethite. The minimum ferrihydrite solubility is at the zero point of charge, near pH 7–8, and this coincides with a hematite maximum at 4°C in an Al-free system (see above). This is consistent with increasing hematite content in the Al-free systems of series 29A from 1–2% hematite at pH 4 to 5–18% hematite at pH 6 and 31% hematite at pH 7.

If the above conclusion is correct, we may assume that Al in ferrihydrite lowers ferrihydrite solubility and thereby favors hematite formation. Note, however, that the strong goethite-excluding effect of Al does not occur in soils, probably because goethite is formed by oxidation of Fe(II). For example, in synthesis experiments using Fe(II) as the Fe source, goethite was the only phase at room temperature (RT) and pH 7, even at high R_i (~0.4 mol mol^{-1}) (Taylor and Schwertmann, 1978; Goodman and Lewis, 1981; Fey and Dixon, 1981).

Properties of hematite

Crystallinity. There are two special features of the XRD patterns of Al-containing hematite, especially at high Al contents. One feature is the pronounced differential line broadening, as illustrated by the broad 104 peak compared to the narrow 110 peak (Figure 3A, traces a and b). The peaks become broader as the function of decreasing angle between the respective *hkl* plane and (001) plane as observed earlier by Perinet and Lafont (1972) and Schwertmann *et al.* (1979). In accordance with TEM observations this is caused by restricted growth along the *c* axis. Unexpectedly, the differential growth is more pronounced with the hematites obtained at 80°C than with those formed at 25°C. Thus, differential growth is favored by rapid crystal growth of Al-containing hematites.

The second feature at high Al content is a high background in the region near the 104 and 110 peaks. In addition to this, an associated weak, broad hump near 0.42 nm (Figure 3A, traces a and d) is not present at low R_s where the hematite is better crystallized (Figure 3A, trace f). Repeated oxalate treatment did not remove these features and Mössbauer spectra (Figure 3B) gave no indication of a second Fe-rich phase, such as of ferrihydrite or goethite. Instead they can be removed by heating the sample at 180°C (Figure 3A, traces b and e). We conclude, therefore, that these features are probably caused by structural OH and/or defects (see below). The broad diffraction hump at 0.42 nm (indexed 101 for hematite) coincides with the 101 peak of goethite. If goethite would be present, the intensity of the diffraction hump would give an amount of ~15% goethite according to the Rietveld simulation. This quantity, however, is easily detected by Mössbauer spectroscopy. We therefore conclude that this peak cannot be goethite. An alternative explanation may be an ordering effect of hydroxyl groups. Locally, this could shift oxygen from the Wyckhoff position 18*e* (*x*, 0, ¼) towards a general position with a concomitant change from space group *R*3*c* to, *e.g.,* *P*31*c*, where a 101 reflection is allowed. Gentle heat-

https://doi.org/10.1346/CCMN.2000.0480202 Published online by Cambridge University Press

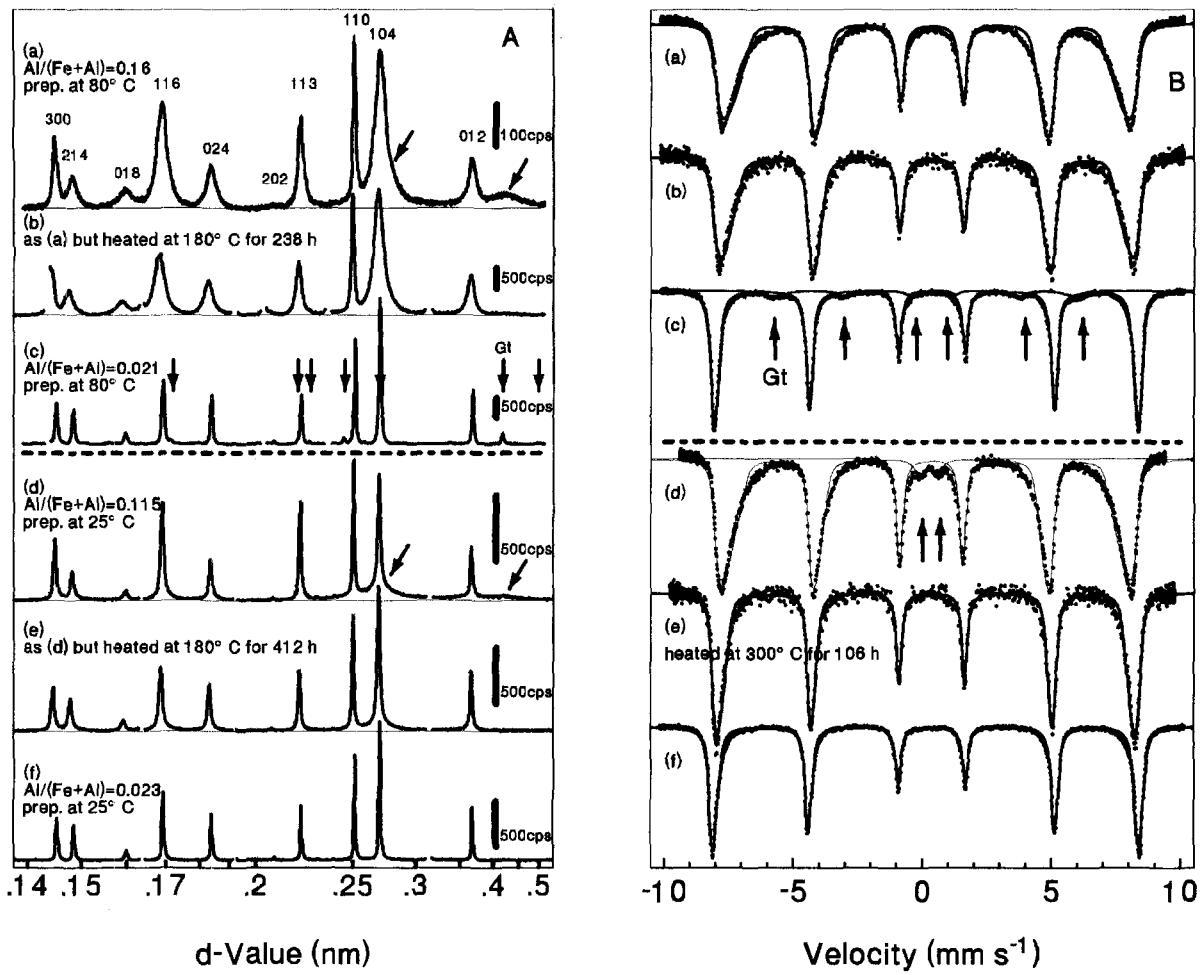

Figure 3. The effect of heating on the XRD patterns (A) and Mössbauer spectra at room temperature (B) of various Al-containing hematites with low and high Al content synthesized at 25 (Series 22A) and 80°C (Series 57).

ing obviously changes this local hydroxyl ordering to a random occupation. Then, the symmetry of the *R*3*c* structure is restored and the broad peak disappears. We stress, however, that this is a preliminary model, requiring additional investigation.

Structural Al in hematite. The structural Al/(Al + Fe) ratio, R_s, of hematite is a function of R_i (Figure 4). The relative incorporation, R_s/R_i, varies with R_i and synthesis temperature. For hematite prepared at 80°C (series 57), R_s/R_i was ~1 over the R_i range of 0–0.15, in agreement with an earlier result for hematite synthesized at 70°C (Schwertmann *et al.,* 1979). In contrast, for hematite synthesized at RT the deviation from the 1:1 line (Figure 4) began at an R_i value <0.15. At an R_i value between 0.15–0.20, R_s even decreased, and for $R_i > 0.20$, the R_s value remained nearly constant at ~0.09 mol mol^{-1}. This drop in R_s value coincided with the appearance of a crystalline $Al(OH)_3$ phase that probably competed with hematite for Al content.

From these results, we conclude that higher synthesis temperatures promote Al incorporation into hematite. This is in contrast to goethite where R_s/R_i was found to decrease from 0.61 to 0.38 as the temperature was raised from 25 to 70°C (Schwertmann and Craciun, unpubl.; see Figure 3.6 in Cornell and Schwertmann, 1996). Thus, at ambient temperature, Al-containing hematite should be less stable and Al-containing goethite should be more stable than the Al-free forms. This is consistent with soils where the Al substitution of hematite is often significantly below half of that of coexisting goethite (Anand and Gilkes, 1987a; Fontes and Weed, 1991; Muller and Boquier, 1987; Singh and Gilkes, 1992; Zeese *et al.,* 1994; Prasetyo and Gilkes, 1994). In 64 hematite-goethite pairs from lateritic duricrusts from Western Australia, Anand and Gilkes (1987b) found that no Al substitution was detected in hematite before the associated goethite had >0.16 mol mol^{-1} Al content. The relatively low Al content of hematite is probably responsible for the

https://doi.org/10.1346/CCMN.2000.0480202 Published online by Cambridge University Press

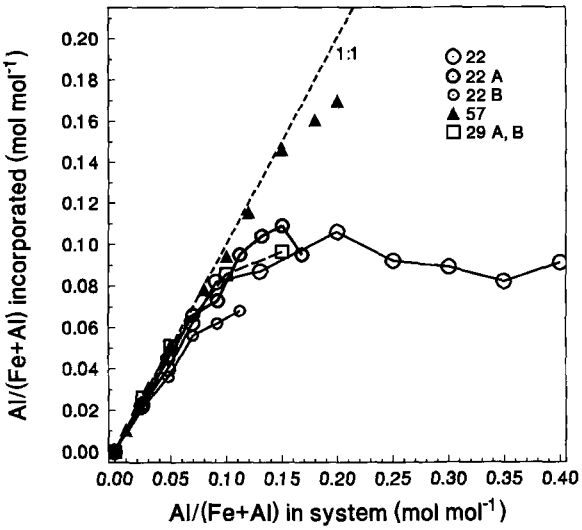

Figure 4. Relationship between structural Al/(Al + Fe) in hematite and the initial Al/(Al + Fe) in the system for hematite synthesized at 25 and 80°C.

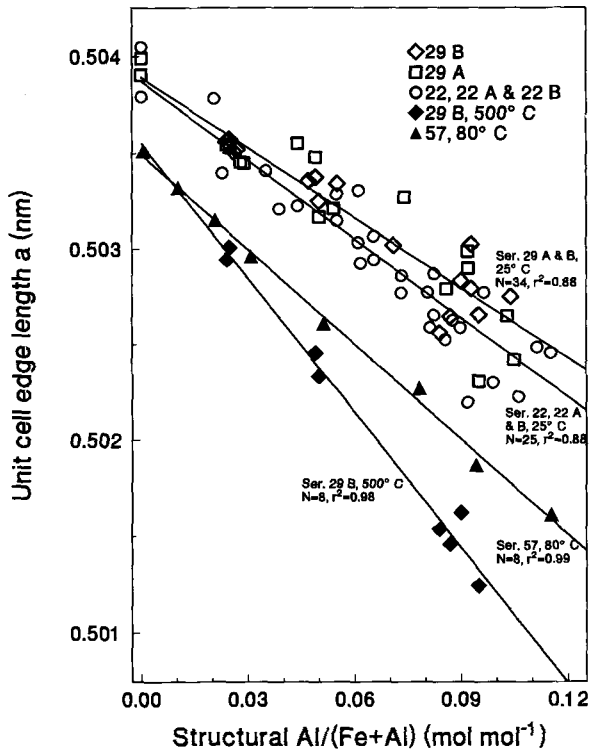

Figure 5. Relationship between the unit-edge length *a* of hematite and structural Al/(Al + Fe).

preferential reductive dissolution of hematite as compared to goethite (Torrent *et al.,* 1987), the well-known yellowing or xanthization process in the upper part of red soils (Macedo and Bryant, 1989; Jeanroy *et al.,* 1991).

Most hematites in soils show Al substitutions of <0.1 mol mol^{-1}, which is observed in our synthesis experiments as well. This Al content is below the maximum possible substitution of 0.16 mol mol^{-1} and reflects the ambient formation temperature. Note, however, that the Al-substitution values for soil hematite are mostly based on a reference curve obtained from hematites synthesized at 70°C. A reference curve based on soil hematites similar to that for soil goethites (Schwertmann and Carlson, 1994) is, thus, needed.

Unit-cell size as influenced by structural Al and OH/H_2O. Figure 5 shows the decrease of the *a* axis of hematite in the five series as a function of the Al content. The relation differs significantly from that of hematite synthesized at higher temperature such as at 70–80°C (Schwertmann *et al.,* 1979; Barron *et al.,* 1984; Kosmas *et al.,* 1986) and even more so for those produced at 1000°C (v. Steinwehr, 1967). Hematites formed at 25°C have larger *a* dimensions at a given R_s, a lower slope (a/R_s), and considerably more scatter in the data (Figure 5). A significant effect of synthesis temperature on the relationship between the *a* axis and structural Al was also noted by Stanjek and Schwertmann (1992). Wolska (1981) and Wolska and Szajda (1985, 1988) suggested structural OH and/or H_2O to be the cause of the above differences and coined the term "hydrohematite" for this phase. Structural OH is probably combined with an equivalent number of Fe vacancies and Wolska and Szajda (1985, 1988) showed that this produces a decrease in the intensities of the 012, 104, 110, and 024 XRD peaks relative to that of the 113 peak which is independent of the Fe occupancy (Wolska, 1981; Stanjek and Schwertmann, 1992). Further support for structural OH was obtained by Wolska and Szajda (1985, 1988) from infrared (IR) spectra. They showed an additional absorption feature at ~950 cm^{-1} and a shoulder at ~650 cm^{-1}, which are both absent in hematite heated to 1000°C. As Al content increases, the band at 950 cm^{-1} moves to lower wave numbers and appears as a shoulder of the Fe-O vibrations (compare Figure 1a with 1b in Wolska and Szajda, 1988). Furthermore, on heating, the feature at 650 cm^{-1} was stable to a higher temperature (>700°C) in the aluminiferrous hematite than in the pure hematite. Our FTIR spectra (Figure 6) agree with those of Wolska and Szajda: both of the above bands are present and heating to 180 and 300°C reduced the intensity of the 950-cm^{-1} band, but did not remove the shoulder at 650 cm^{-1}. These results support the presence of OH.

For further support, an Al-containing hematite with R_s of 0.11 was heated sequentially to 70, 100, 180, 240, and 300°C until constant weight was obtained for each temperature. Between 100–180°C the loss on heating increased abruptly (Figure 7a) and the cell lengths *a* and *c* (Figure 7b) and thus, the volume, decreased. The *a* axis now occurs on the line for the

https://doi.org/10.1346/CCMN.2000.0480202 Published online by Cambridge University Press

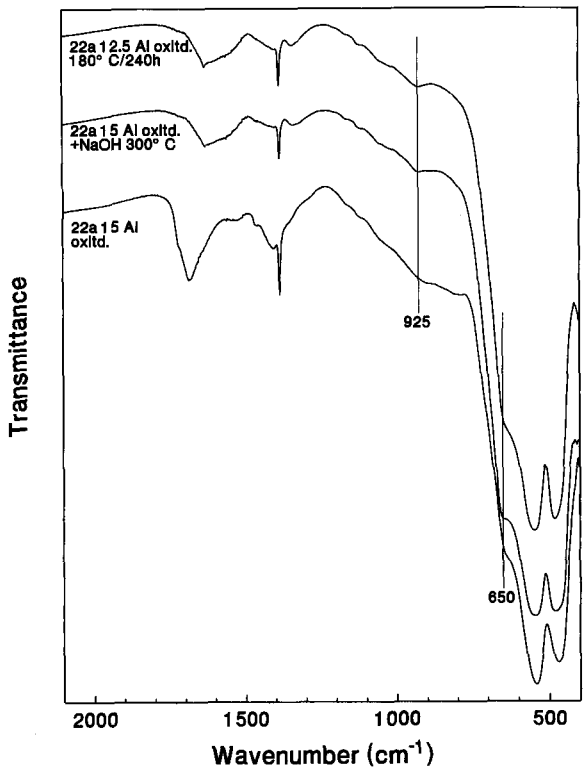

Figure 6. FTIR spectra of Al-containing hematite with an Al/(Al + Fe) ratio of 0.103 mol mol^{-1} (22A-15) before and after heating at 180 (238 h) and 300°C (1084 h). The sharp peak at ~1400 cm^{-1} is caused by a trace of residual nitrate.

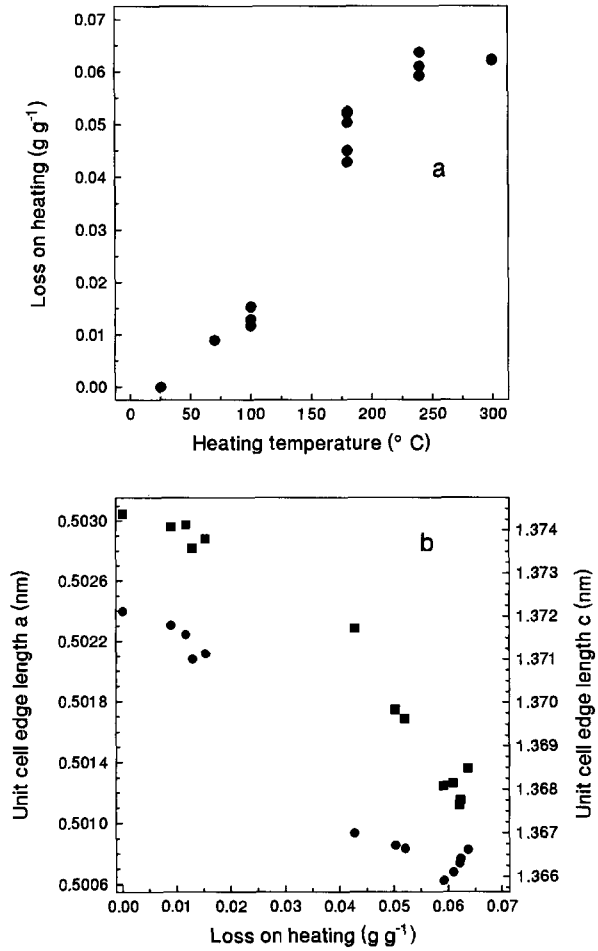

Figure 7. Al-containing hematite with Al/(Al + Fe) of 0.11 mol mol^{-1}. Relationship between heating temperature and weight loss (a) and between unit length *a* (●) and *c* (■) and weight loss (b).

hematites synthesized at 500°C (compare Figure 7b with Figure 5). Structural defects, especially vacant octahedral sites, charge balanced by OH and Al-OH groups are then essentially removed. Transmission electron micrographs (not shown) indicate no changes in external crystal morphology even after heating stepwise to 300°C. Hematite of a complete Al series (22A) heated for 238 h at 180°C consistently showed that after heating the reduction in *a* was greater with the higher R_s (Figure 8).

Hyperfine properties as influenced by structural Al and OH/H$_2$O. At 4.2 K the mean hyperfine field, B_{hf}, of the fraction not having passed the Morin transition was in the range of 53.0–53.3 Tesla (T) for samples both before and after heating at 500°C for 16 h (Figure 9). A small systematic lowering effect of structural Al on B_{hf} as previously described for hematite synthesized at high temperatures (De Grave *et al.*, 1988) is probably obscured by OH or defects in the structure. No Morin transition was observed at $R_s > 0.025$ for unheated hematite and at >0.05 for hematite heated at 500°C.

The Mössbauer spectra at RT were dominated by magnetic sextets. The width and asymmetry of the lines increased with increasing structural Al (Figure 3B: compare trace a with trace c and trace d with trace f), whereas B_{hf} decreased from 50 to 44 T (Figure 9). Note from Figure 3B, trace c, a small amount of goethite at low R_s is clearly visible in the spectrum, in agreement with XRD results. On heating the 22A samples to 180°C (Figure 3B, trace b) and to 300°C (Figure 3B, trace e), B_{hf} increased significantly from 47.5 to 49.6 T, whereas heating the 29B samples to 500°C resulted in a smaller increase positively related to structural Al (Figure 9). Thus, the depressive effect of structural OH on B_{hf} enhances that of Al. This also becomes evident from the appearence of a doublet beginning with an R_i of 0.15 (intensity ~4%) which increases with R_s (R_s = 0.175: ~7%; R_s = 0.20: 18%) indicating that part of the hematite was no longer magnetically ordered at RT or, more likely, in the superparamagnetic state. It is unlikely that the doublet has a contribution from ferrihydrite because the intensity remained unaltered after treating the hematites repeat-

https://doi.org/10.1346/CCMN.2000.0480202 Published online by Cambridge University Press

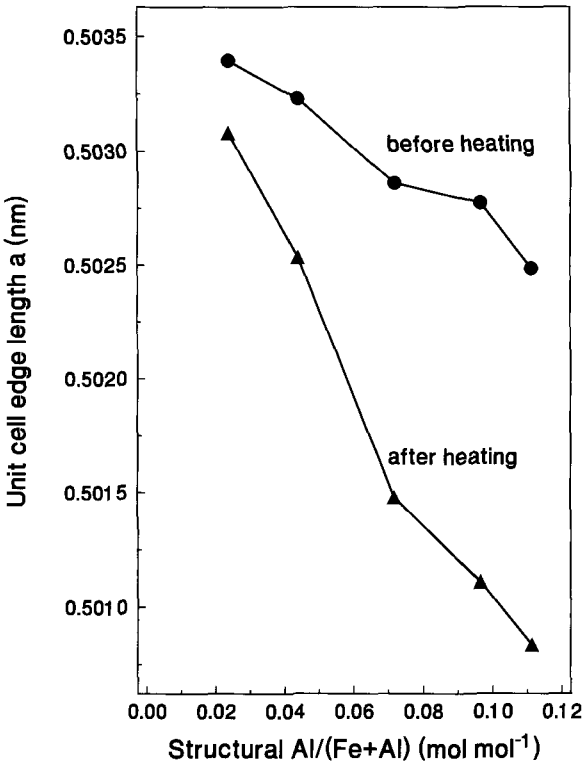

Figure 8. Reduction of unit length *a* of Al-containing hematite (Series 22A) caused by heating for 238 h at 180°C.

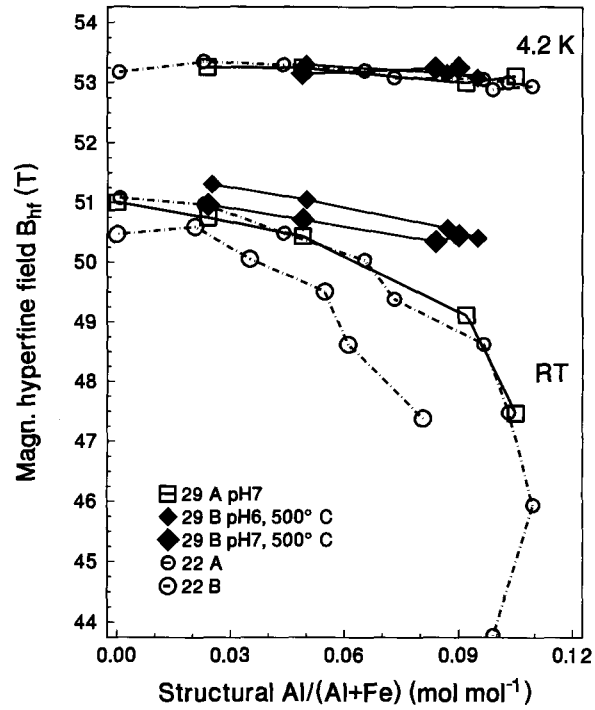

Figure 9. Relationship between the magnetic hyperfine field at room temperature and 4.2 K and structural Al/(Al + Fe) in hematite.

edly with oxalate or 0.1 M HCl. The intensity increased, however, from 3.8 to 4.6% when the sample (29A-15) was measured twice at 22 and at 26°C. After heating the samples to 500°C, the B_{hf} values increased and coincided with values reported by De Grave *et al.* (1982), showing that any influence of structural OH and defects, which may be inherently correlated with Al substitution in hematites prepared at low or ambient temperature, had been removed.

Crystal shape and size, surface area, and micropore volume. Crystal shape and, to a lesser extent, crystal size varies with Al and pH in the system. As R_i increases, crystal shape changes drastically from hexagonal or rhombohedral with smooth edges and homogeneous interiors (Figure 10a and 10b) to disks or framboids with rough edges and grainy interiors (Figure 10c–10f). The crystal diameter is ~100 nm with somewhat larger crystals occurring at pH 6 and 7 (Figure 10c). Hematite crystals with grainy interiors were also reported from soils (Schwertmann and Kämpf, 1985; Anand and Gilkes, 1987b; de Brito Galvão and Schulze, 1996). The disk-shaped crystals lie mostly on flat sides, but some appear to stand on edge (Figure 10c). From these crystals, it is obvious that they are thicker in the center than at the edges and that they have a layer-like internal structure. This is also observed in crystals lying on their flat side by a stepwise increase of opacity towards the center (see arrows). A view of the disks was obtained with SEM (Figure 11), from which a maximum thickness of 50–65 nm was determined, in agreement with TEM. Figure 11 also illustrates the gradual transition from rhombohedral to discoid crystals with increasing Al substitution. In comparison, the highly substituted hematite crystals synthesized at 80°C have no regular shape and appear extremely thin (Figure 12). This agrees with the extreme differential line broadening (Figure 3A, trace a) and suggests that the rate of formation, which is much higher at 80°C than at 25°C, determines the anisotropy more strongly than synthesis temperature.

Structural Al influenced both the mean coherence length along *a* and *c* (MCL_a; MCL_c) (Figure 13). As R_s increased from 0.025 to ~0.1, MCL_c decreased by ~20 nm whereas MCL_a did not change significantly. We propose that OH, incorporated into the structure as a consequence of Al substitution, rather than the presence of Al itself, caused the loss in MCL_c. The weak MCL maximum at low R_s confirms earlier results obtained with hematites synthesized at 70°C, that some strain relief occurs when small amounts of Al are incorporated into the hematite structure (Schwertmann *et al.*, 1979). In comparison with the crystal size observed from TEM, the MCL values are significantly smaller. Variations may be related to the full line width, which is attributed to particle-size broadening,

https://doi.org/10.1346/CCMN.2000.0480202 Published online by Cambridge University Press

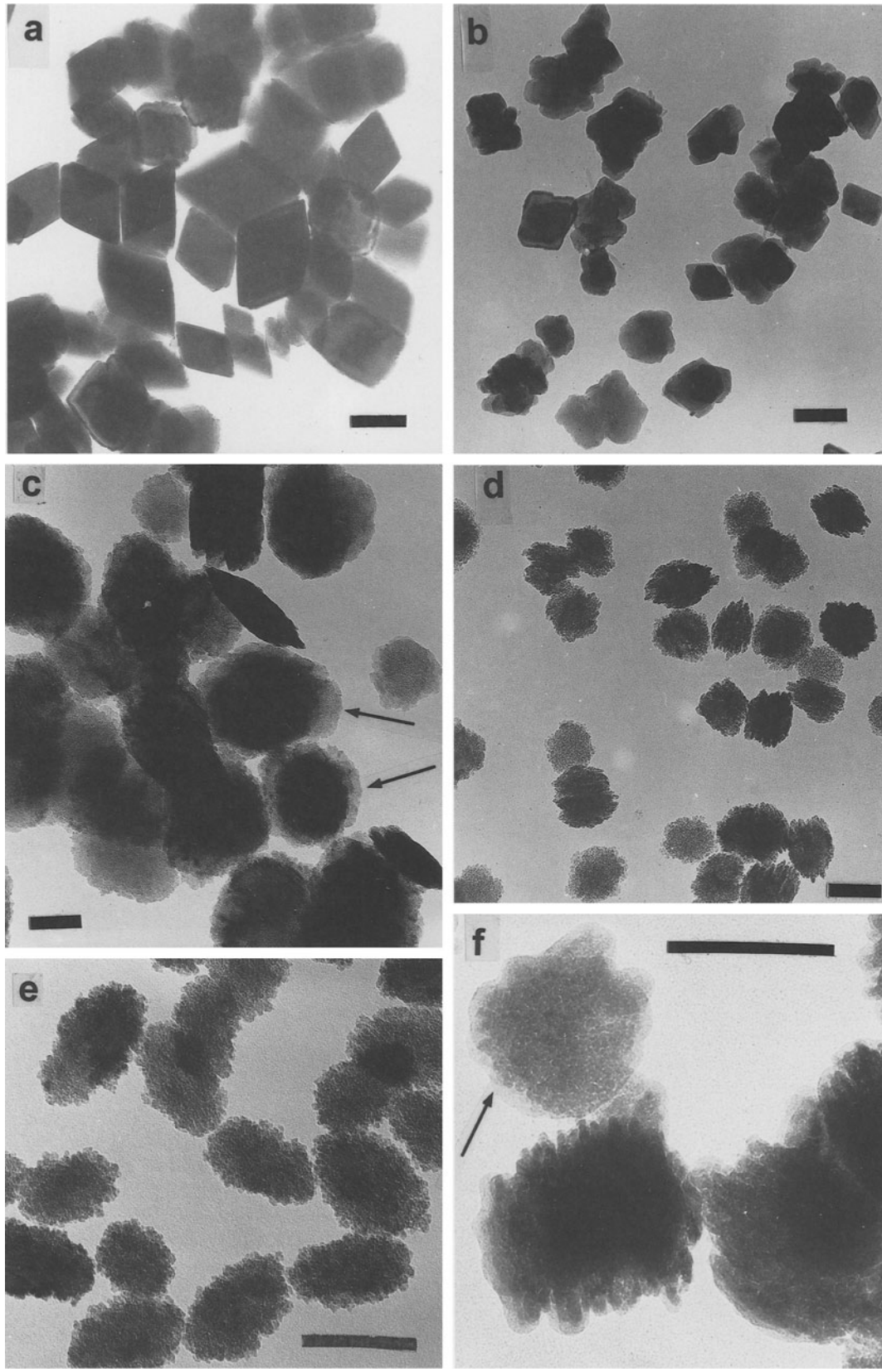

https://doi.org/10.1346/CCMN.2000.0480202 Published online by Cambridge University Press

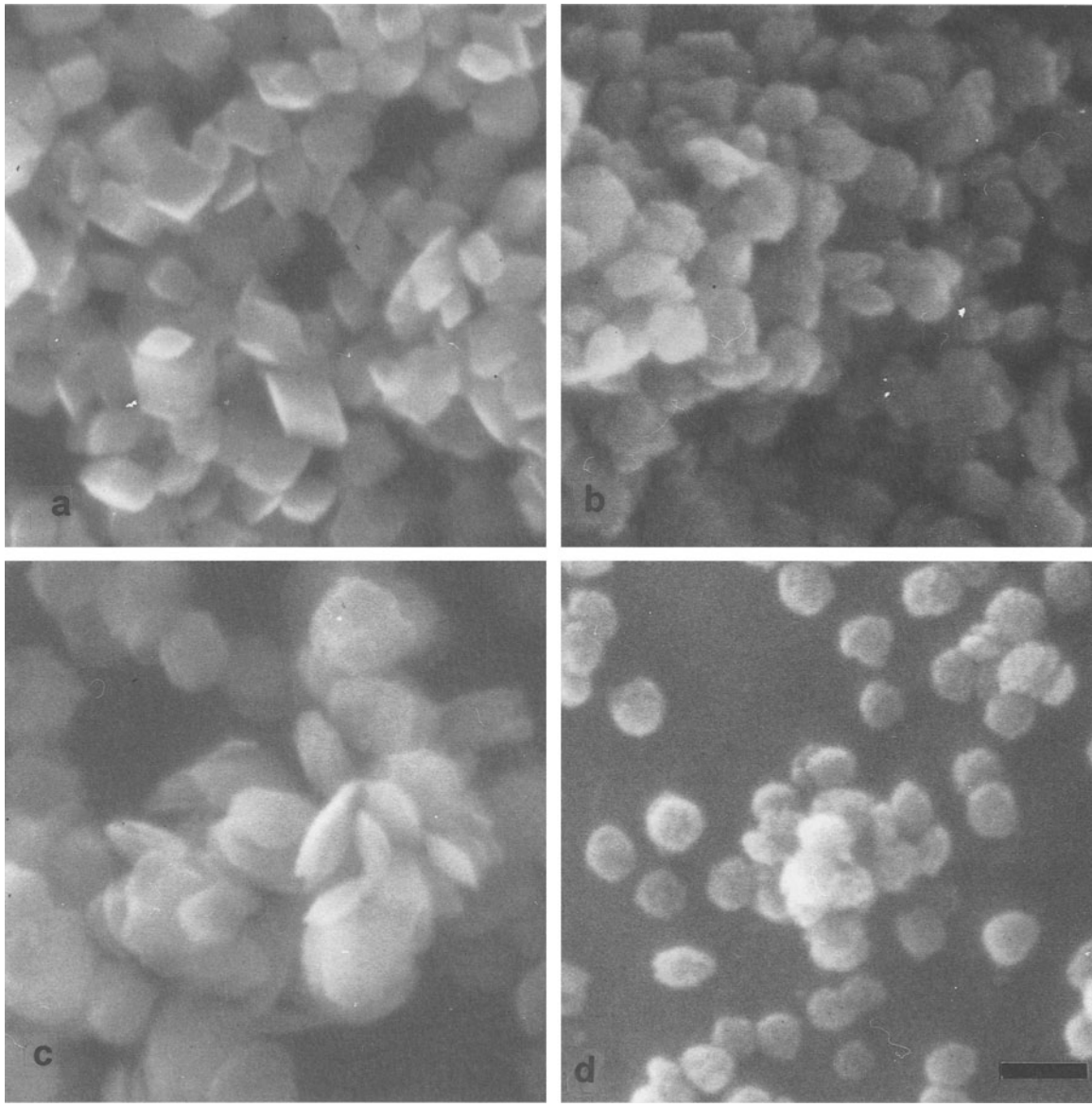

Figure 11. Scanning electron micrographs of Al-containing hematites: (a) Series 22A, R_i 0.05, pH 7; (b) Series 29A, R_i 0.05, pH 7; (c) Series 29A, R_i 0.10, pH 7; (d) Series 29A, R_i 0.15, pH 5. The bar is 0.2 μm.

whereas part of the width may originate from strain. Although grainy in their interior, TEM images do not indicate domains along *a*. In contrast, 4–8-nm thick domains are visible along *c* (Figure 10d and 10f). The MCL_a and MCL_c values did not increase substantially after stepwise heating to 300°C (not shown) nor after heating to 500°C (Figure 13). This shows that the removal of structural OH improves structural order but does not enlarge structural coherence. A change in coherence may require sintering temperatures.

In contrast to expectations from TEM observations, the surface area (BET) *in*creased rather than decreased with increasing crystal diameter, *i.e.,* with increasing Al content (Figure 14). This apparent discrepancy can be explained both by the thinness and surface roughness of the discoid crystals at high Al substitution

←

Figure 10. Transmission electron micrographs of Al-containing hematite with various crystal morphology [Series 29A, except (a) which is from Series 22A] [R_i = Al/(Al + Fe) for the system]: (a) R_i 0.05, pH 7; (b) R_i 0.025, pH 7; (c) R_i 0.10, pH 7; (d) R_i 0.15, pH 5; (e) R_i 0.15, pH 4; (f) R_i 0.15, pH 5. The bar is 100 nm.

https://doi.org/10.1346/CCMN.2000.0480202 Published online by Cambridge University Press

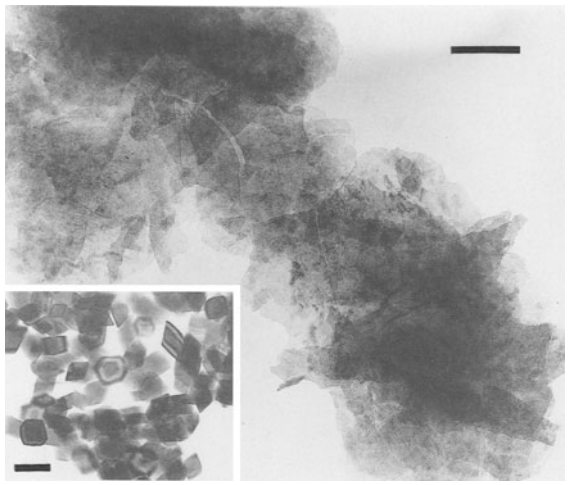

Figure 12. Transmission electron micrographs of Al-containing hematite synthesized at 80°C (Series 57) with Al/(Al + Fe) = 0.18 as compared to Al/(Al + Fe) = 0.02 (insert). The bar is 100 nm.

compared to the smooth, rhombohedral crystals at low Al substitution. This is also consistent with an increase in micropore volume and micropore surface as a proportion of total surface as structural Al increased (Figure 14).

CONCLUSIONS

The long-term transformation of Al-containing 2-line ferrihydrite under ambient conditions with respect to temperature and pH resulted in Al-containing hematites resembling soil hematites. One similarity is crystal morphology, but it is inconclusive if the decrease in unit-cell size by structural Al is also counteracted by structural hydroxyl (or water). Therefore, the relationship between unit-cell edge length and Al content of Al-containing hematites synthesized at elevated temperatures (*e.g.,* 70°C) may not provide an accurate assessment of Al substitution of soil hematites. Preheating to ~200°C before using XRD or Mössbauer spectroscopy may overcome this problem.

A feature of soil Fe oxides that cannot be explained by our results is the following: In many soils highly substituted goethite coexists in an intimate mixture with Al-containing hematite, whereas in synthesis experiments Al suppressed goethite formation. This result may be related to a different way that hematite forms in soils, namely from an Fe(II) system rather than from ferrihydrite. Thus far, the Fe(II) system has only been used for goethite and lepidocrocite synthesis. Whether hematite can also be formed from an Fe(II) system warrants additional study.

ACKNOWLEDGMENTS

Series 22 was installed by D.G. Lewis while on sabbatical leave from the Department of Soil Science, The University of Adelaide, South Australia. We gratefully acknowledge the help of W. Knapp and H.-Ch. Bartscherer, Physik Weihenstephan, for the many TEM and SEM micrographs, G. Pfab, U. Maul, and B. Kremer for skillful preparatory and analytical work, F.E. Wagner, Physics Department, Garching, for enabling Mössbauer spectra to be taken at 4.2 K, and E. Murad, Bamberg, for the FTIR spectra. We also thank J.E. Amonette, P.L. Gassman, R.J. Gilkes, and S. Guggenheim for providing helpful comments for improving the paper.

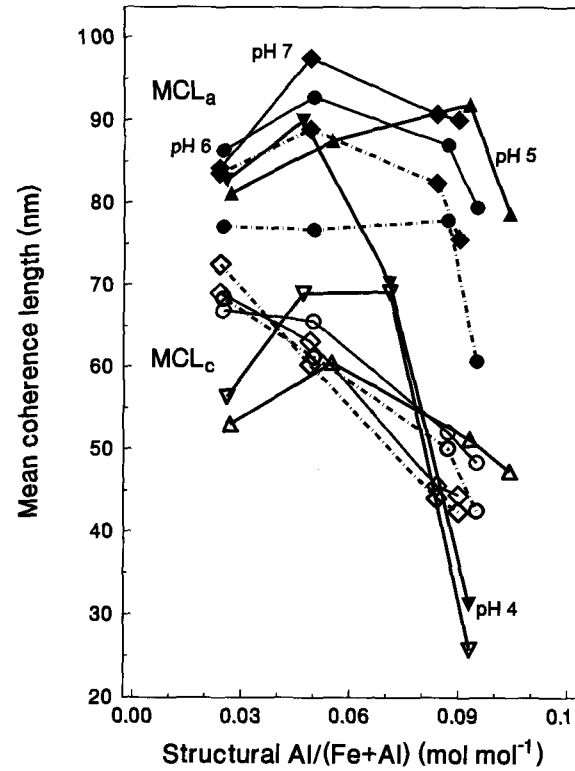

Figure 13. Relationship between MCL_a (upper) and MCL_c (lower) and structural Al before (solid lines) and after heating (broken lines) at 500°C.

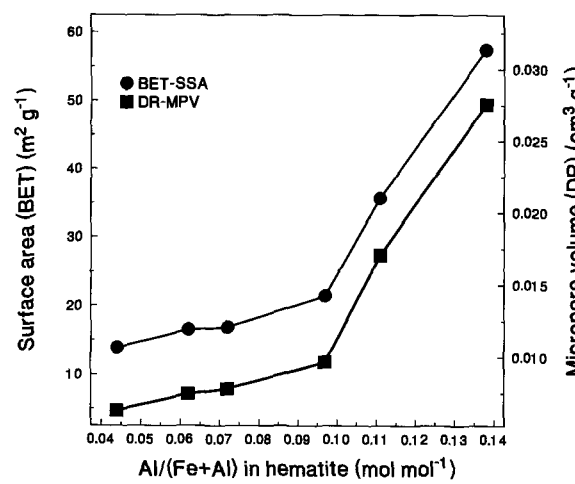

Figure 14. Relationship between Al in hematite and its surface area and micropore volume.

https://doi.org/10.1346/CCMN.2000.0480202 Published online by Cambridge University Press

REFERENCES

Anand, R.R. and Gilkes, R.J. (1987a) Variation in the properties of iron oxides within individual specimens of lateritic duricrust. *Australian Journal of Soil Research,* **25,** 287–302.

Anand, R.R. and Gilkes, R.J. (1987b) Iron oxides in lateritic soils. *Journal of Soil Science,* **38,** 607–622.

Atkinson, R.J., Posner, A.M., and Quirk, J.P. (1968) Crystal nucleation in Fe(III) solutions and hydroxide gels. *Journal of Inorganic and Nuclear Chemistry,* **30,** 2371–2381.

Barron, V., Rendon, J.L., Torrent, J., and Serna, C.J. (1984) Relation of infrared, crystallochemical, and morphological properties of Al-substituted hematites. *Clays and Clay Minerals,* **32,** 475–479.

Cornell, R.M. and Schwertmann, U. (1996) *The Iron Oxides.* VCH, Weinheim, 573 pp.

de Brito Galvão, T.C. and Schulze, D.G. (1996) Mineralogical properties of a collapsible lateritic soil from Minas Gerais, Brazil. *Soil Science Society of America Journal,* **60,** 1969–1978.

De Grave, E., Bowen, L.H., and Weed, S.B. (1982) Mössbauer study of aluminum-substituted hematites. *Journal of Magnetic Materials,* **27,** 98–108.

De Grave, E., Bowen, L.H., Vochten, R., and Vandenberghe, R.E. (1988) The effect of crystallinity and Al substitution on the magnetic structure and Morin transition in hematite. *Journal of Magnetic Materials,* **72,** 141–151.

Fey, M.V. and Dixon, J.B. (1981) Synthesis and properties of poorly crystalline hydrated aluminous goethites. *Clays and Clay Minerals,* **29,** 91–100.

Fischer, W.R. and Schwertmann, U. (1975) The formation of hematite from amorphous iron(III)-hydroxide. *Clays and Clay Minerals,* **23,** 33–37.

Fontes, M.P.F. and Weed, S.B. (1991) Iron oxides in selected Brazilian oxisols: I. Mineralogy. *Soil Science Society of America Journal,* **55,** 1143–1149.

Friedl, J. and Schwertmann, U. (1996) Aluminium influence on iron oxides: XVIII. The effect of Al substution and crystal size on magnetic hyperfine fields of natural goethites. *Clay Minerals,* **31,** 455–464.

Glasauer, S., Friedl, J., and Schwertmann, U. (1999) Properties of goethite prepared in acid and basic conditions in the presence of silicate. *Journal of Interface and Colloid Science,* **216,** 106–115.

Goodman, B.A. and Lewis, D.G. (1981) Mössbauer spectra of aluminous goethites (α-FeOOH). *Journal of Soil Science,* **32,** 351–363.

Izumi, F. (1993) Rietveld analysis programs RIETAN and PREMOS and special applications. In *The Rietveld Method,* R.A. Young, ed., Oxford University Press, Oxford, 236–253.

Jeanroy, E., Rajot, J.L., Pillon, P., and Herbillon, A.J. (1991) Differential dissolution of hematite and goethite in dithionite and its implications on soil yellowing. *Geoderma,* **50,** 79–94.

Kosmas, C.S., Franzmeier, D.P., and Schulze, D.G. (1986) Relationship among derivative spectroscopy, color, crystallite dimensions and Al substitution of synthetic goethites and hematites. *Clays and Clay Minerals,* **34,** 625–634.

Lewis, D.G. and Schwertmann, U. (1980) The effect of (OH) on the goethite produced from ferrihydrite under alkaline conditions. *Journal of Colloid Interface Science,* **78,** 543–553.

Macedo, J. and Bryant, B.B. (1989) Preferential microbial reduction of hematite over goethite in a Brazilian oxisol. *Soil Science Society of America Journal,* **53,** 1114–1118.

Muller, J.-P. and Boquier, G. (1987) Textural and mineralogical relationships between ferruginous nodules and surrounding clayey matrix in a laterite from Cameroon. In *Proceedings of the International Clay Conference, Denver,* L.G. Schultz, H. van Olphen, and F.A. Mumpton, eds., The Clay Minerals Society, Bloomington, Indiana, 184–194.

Perinet, G. and Lafont, R. (1972) Sur les parametres cristallographiques des hematites alumineuses. *Contes Rendue Academie de Science,* **275,** 1021–1024.

Prasetyo, B.H. and Gilkes, R.J. (1994) Properties of iron oxides from red soils derived from tuff in western Java. *Australian Journal of Soil Research,* **32,** 781–794.

Schneider, J. and Dinnebier, R.E. (1991) GUFI-WYRIET: An integrated PC powder pattern analysis package. *Material Science Forum,* **79–82,** 277–282.

Schulze, D.G. and Schwertmann, U. (1987) The influence of aluminium on iron oxides. XIII. Properties of goethites synthesized in 0.2 M KOH at 25°C. *Clay Minerals,* **22,** 83–92.

Schwertmann, U. (1964) Differenzierung der Eisenoxide des Bodens durch Extraktion mit Ammoniumoxalat-Lösung. *Zeitschrift für Pflanzenernährung, Düngung und Bodenkunde,* **105,** 194–202.

Schwertmann, U. (1988) Goethite and hematite formation in the presence of clay minerals and gibbsite at 25°C. *Soil Science Society of America Journal,* **52,** 288–291.

Schwertmann, U. and Carlson, L. (1994) Aluminum influence on iron oxides: XVII. Unit cell parameters and aluminum substitution of natural goethites. *Soil Science Society of America Journal,* **58,** 256–261.

Schwertmann, U. and Cornell, R.M. (1991) *Iron Oxides in the Laboratory.* VCH, Weinheim, 119 pp.

Schwertmann, U. and Kämpf, N. (1985) Properties of goethite and hematite in kaolinitic soils of southern and central Brazil. *Soil Science,* **139,** 344–350.

Schwertmann, U. and Murad, E. (1983) Effect of pH on the formation of goethite and hematite from ferrihydrite. *Clays and Clay Minerals,* **31,** 277–284.

Schwertmann, U., Fitzpatrick, R.W., Taylor, R.M., and Lewis, D.G. (1979) The influence of aluminum on iron oxides. Part II. Preparation and properties of Al-substituted hematites. *Clays and Clay Minerals,* **27,** 105–112.

Schwertmann, U., Friedl, J., and Stanjek, H. (1999) From Fe(III) ions to ferrihydrite and then to hematite. *Journal of Colloid and Interface Science,* **209,** 215–223.

Singh, B. and Gilkes, R.J. (1992) Properties and distribution of iron oxides and their association with minor elements in the soils of south-western Australia. *Journal of Soil Science,* **43,** 77–98.

Stanjek, H. and Schwertmann, U. (1992) The influence of aluminum on iron oxides. Part XVI: Hydroxyl and aluminum substitution in synthetic hematites. *Clays and Clay Minerals,* **40,** 347–354.

Steinwehr, H.E. von (1967) Ursachen der Abweichung von der Vegard' schen Regel. *Zeitschrift für Kristallographie,* **1235,** 360–376.

Taylor, R.M. (1988) Proposed mechanism for the formation of soluble Si–Al and Fe(III)–Al hydroxy complexes in soils. *Geoderma,* **42,** 65–77.

Taylor, R.M. and Schwertmann, U. (1978) The influence of aluminum on iron oxides. I. The influence of Al on Fe oxide formation from the Fe(II) system. *Clays and Clay Minerals,* **26,** 373–383.

Torrent, J., Schwertmann, U., and Barron, V. (1987) The reductive dissolution of synthetic goethite and hematite in dithionite. *Clay Minerals,* **22,** 329–337.

Wolska, E. (1981) The structure of hydrohematite. *Zeitschrift für Kristallographie,* **154,** 69–75.

https://doi.org/10.1346/CCMN.2000.0480202 Published online by Cambridge University Press

Wolska, E. and Szajda, W. (1985) Structural and spectroscopic characteristics of synthetic hydrohematite. *Journal of Material Science,* **20,** 4407–4414.

Wolska, E. and Szajda, W. (1988) The effect of cationic and anionic substitution on the α-$(Al, Fe)_2O_3$ lattice parameters. *Solid State Ionics,* **28–30,** 1320–1323.

Zeese, R., Schwertmann, U., Tietz, G.F., and Jux, U. (1994) Mineralogy and stratigraphy of three deep lateritic profiles of the Jos plateau, Central Nigeria. *Catena,* **21,** 195–214.

E-mail of corresponding author: uschwert@pollux.edv.agrar.tu-muenchen.de

(*Received 1 February 1999; accepted 17 September 1999; Ms. 308; A.E. James E. Amonette*)

https://doi.org/10.1346/CCMN.2000.0480202 Published online by Cambridge University Press